On the Free Radical Redox Chemistry of 5,6-Dihydroxyindole

A. Bernardus Mostert [a*]

[a] Department of Chemistry, Swansea University, Singleton Park, SA2, 8PP, Wales, UK

* a.b.mostert@swansea.ac.uk

Highlights

- Redox equations for *o*-quinone systems with quinone methide formation are presented.
- Holistic thermodynamic model for 5,6-dihydroxyindole.
- First estimations of key chemical thermodynamical parameters for 5,6-dihydroxyindole.
- Enhanced understanding of poly-indolequinones such as poly-dopamine and melanin.

Abstract

The poly-indolequinone polymers such as poly-dopamine and melanin are significant materials for advanced soft materials in coatings and devices. In order to make progress towards a holistic thermodynamic model, one can consider the thermodynamics of the redox chemistry of a key monomer building block: 5,6-dihydroxyindole. The work presented here indicates a new observation, that the quinone methide tautomer plays a key role in semiquinone free radical production. The modelling includes a new set of pH dependent, reduction potential equations to account for tautomerisation. Furthermore, presented are estimations for various thermodynamic variables. The 1 electron potential for the quinone reduction is between 0.14 to 0.17 V (NHE); Semiquinone reduction is between -0.10 to -0.068 (NHE); Tautomarisation constant is estimated to be 0.99 to 3.9; Comproportionation formation constant is estimated to be between 3.8×10^3 and 50×10^3. The work presented here may form the basis for understanding the charge transport properties for poly-indolequinones.

Keywords

5,6-dihydroxyindole; melanin; poly-dopamine; redox chemistry; quinone methide; thermodynamic models

1. Introduction

The poly-indolequinone polymers such as poly-dopamine and the melanins have seen an explosion of interest in the past decade due to their potential application ranging from multifunctional coatings to functional materials in devices and sensors.[1] [2] [3] This wide range of application is due to the versatility of these polymers and their properties which include hydrophobic and hydrophilic surface adhesion,[4] [5] [6] [7] [8] stable free radicals, [9] hygroscopic properties[10] [11] and conductive properties[12] to name a few.

Poly-dopamine has been at the forefront of materials design and application, but, as a material per se, it has not received as much attention as its sister compound, eumelanin. Eumelanin, the brown-black pigment found in human skin, commonly referred to just as melanin, has a deeper knowledge base of its basic properties, and hence is a good class to study the poly-indolequinone polymers. Melanin acts as a photo-protectant against harmful UV radiation, and is synthesized from two main monomers: 5,6-dihydroxyindole (DHI) and 5,6-dihydroxyindole-2-carboxylic acid (DHICA) and their various redox forms (Figure 1).[12] [13] [14] [15] Melanin is also in other parts of the body including the *substantia nigra* of the brain stem[16] (combined with pheomelanin to form neuromelanin[17]) and the eye,[18] where the exact biological roles are still somewhat uncertain. Melanin has a range of interesting physico-chemical properties including broad-band optical absorption;[19] robustness towards exposure to harmful radiation;[20] almost complete non-radiative conversion of absorbed photon energy;[21] hygroscopic properties;[10] [22] [11] [23] stable free radical properties;[24] [25] [26] [22] [27] [28] and conductive properties,[29] [30] [28] [22] [24] [31] [32] [33] all of which are exploited to some extent in devices and material applications.[34] [35] [36] [37] [38] [32]

The aforementioned free radical and conductive properties are intimately linked by radical/redox chemistry.[31] [24] [14] [8] [39] [28] [29] For example, melanin's conductivity is dependent upon the degree of hydration, which is modulated by a comproportionation redox reaction (Figure 2a).[24] [22] [28] [29] In short, a chemical self-doping effect occurs whereby one-electron oxidation of the catechol (reduction of the quinone) to the semi-quinone releases protons into the hydrating water matrix.

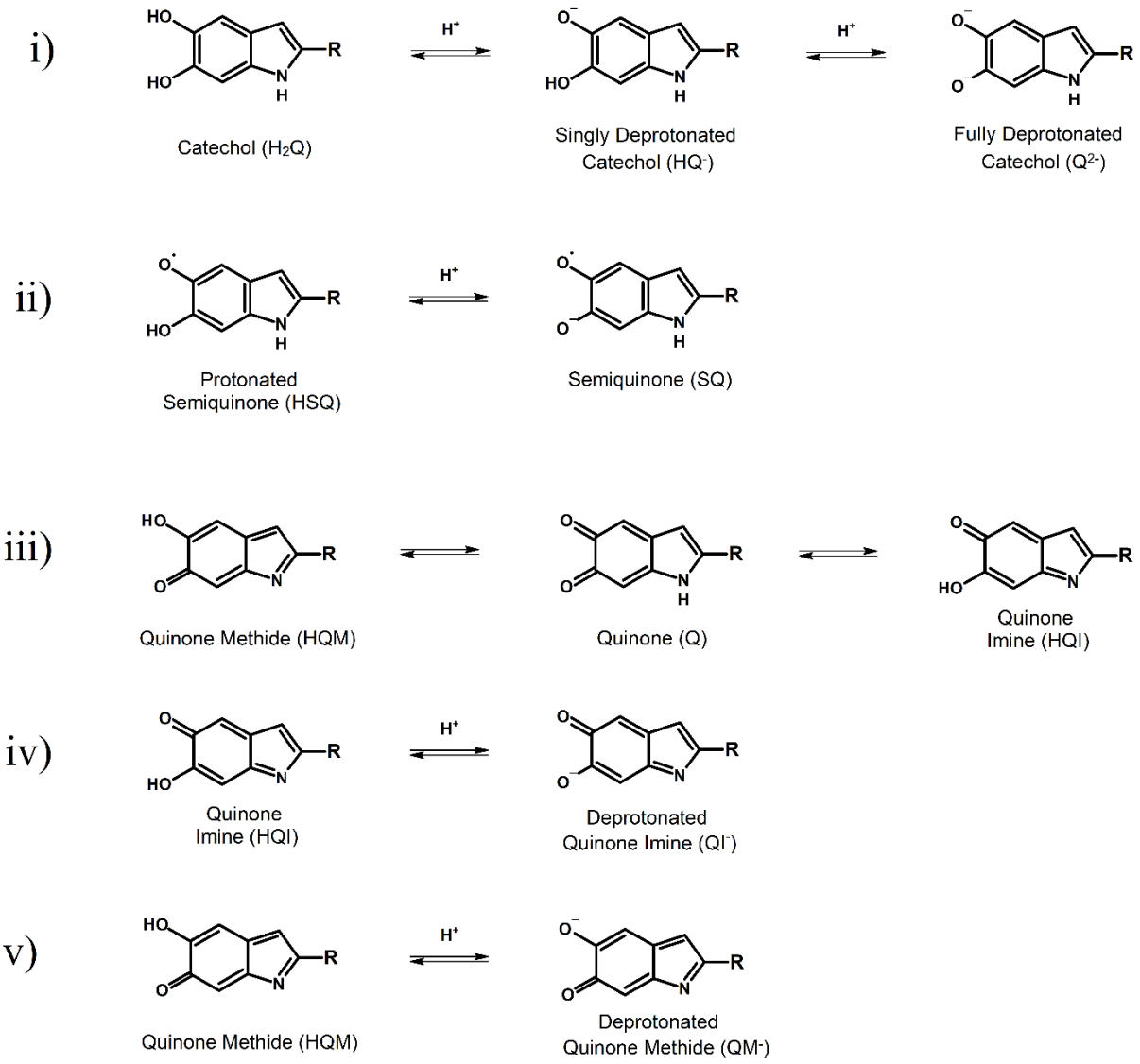

Figure 1: The starting monomers of melanin and their various redox states and tautomers. i) For the hydroquinone catechol where R = H, one has a 5,6-dihydroxyindole (DHI). For R = COOH one obtains a 5,6-dihydroxyindole-2-carboxylic acid (DHICA). These two molecules are the primary starting monomers for melanin synthesis. The molecules listed below, ii) – iv), are various redox states of DHI and DHICA in increasing oxidation with associated deprotonation reactions (i, ii, iv & v). Also included are the tautomerisation reactions of the quinone to quinone imine and quinone methide (iii).

It is clear from the literature that the physical and chemical properties of melanin and the poly-dopamine systems are interpreted to a major extent on the underlying DHI & DHICA moiety chemistry. However, currently no holistic thermodynamic model exists for poly-indolequinones, nor even for the simplest molecule DHI. Given the interest in these materials, it is imperative to understand the nature of the free radical/redox properties as determined by thermodynamic reality. It is therefore the purpose of this paper to begin rectifying the problem by using the published electrochemical data of DHI to generate a simple thermodynamic model as a starting point. The hope is that the modelling and explanations presented here would form a foundation

for more advanced work, thus enabling theoretical predictions of properties of poly-indolequinone systems such as, for example, their conductivity behavior.

2. Methods and Theory

2.1. Background to Theory

In order to model the DHI molecular system, we will assume that the molecular system is in a solution of water in the ideal-dilute limit, in line with much of the experimental work that has been published on DHI. The above assumptions, as will be seen, lead to a reasonable model and allow additional insight into the underlying chemistry of DHI.

It is worth going through the basic chemistry reactions in order to understand the development of the theory for modelling. DHI has 3 oxidation states: a catechol or DHI proper, a semiquinone, and a quinone which is the highest oxidative state. These are depicted in Figure 1. These separate entities can all undergo protonation/deprotonation, which implies an associated pK_a.

To enable interconversion between the various oxidative states, one has to include the potential redox reactions (see Figure 2). The necessary reactions to be included are the 1 electron reduction (oxidation) reactions of the quinone (semiquinone) and of the semiquinone (deprotonated catechol, Q^{2-}). These two reactions can be combined together to describe the 2 electron reduction (oxidation) of the quinone (deprotonated catechol, Q^{2-}) and the comproportionation reaction. These redox reactions can also be described when in the presence of protons, as depicted in Figure 2c.

We now turn to tautomerisation reactions, which yield different forms of the quinone moiety, and, as will be seen in the results section, is an important reaction to consider. As depicted in Figure 1iii), the quinone can tautomerise to either a quinone methide or a quinone imine.[40] [41] [42] A question to ask is which of the two tautomers would be preferred or whether they are equally likely. Computational work on various monomers of DHI, accounting for a water solvent,[43] [44] indicate that the quinone is the more stable entity, followed by the methide (energy ~8.0 kcal mol^{-1}[43] / ~6.0 kcal mol^{-1} [44] above the quinone) and finally the imine (energy ~12 kcal mol^{-1} [43] / >6.2 kcal mol^{-1} [44] above the quinone). As such, the effects of hydrogen bonding from the water solvent on the stability of the various tautomers are also accounted for. Overall, these

results would indicate that the methide is the preferred tautomer and that the quinone imine would be unstable[44] in water. This observation appears to be confirmed by considering that melanogenesis from DHI into melanin occurs via the quinone methide, which appears to be present and not the quinone imine.[40] [41] [42] Overall, it is clear that tautomerisation needs to be accounted for, but only the quinone methide (and its deprotonation) will be considered viable while the quinone imine will be discounted. This brings us to the work of Spoganicz *et al*.[45], who originally advanced the idea of tautomerisation for DHI and proposed the quinone imine as the likely system. These authors never considered the methide as an alternative tautomer. A closer inspection of their work does not inherently presuppose the imine over the methide. As a result, in light of the above discussion, this work uses the results of Spoganicz *et al*.[45], with the caveat that the tautomerisation leads to the methide.

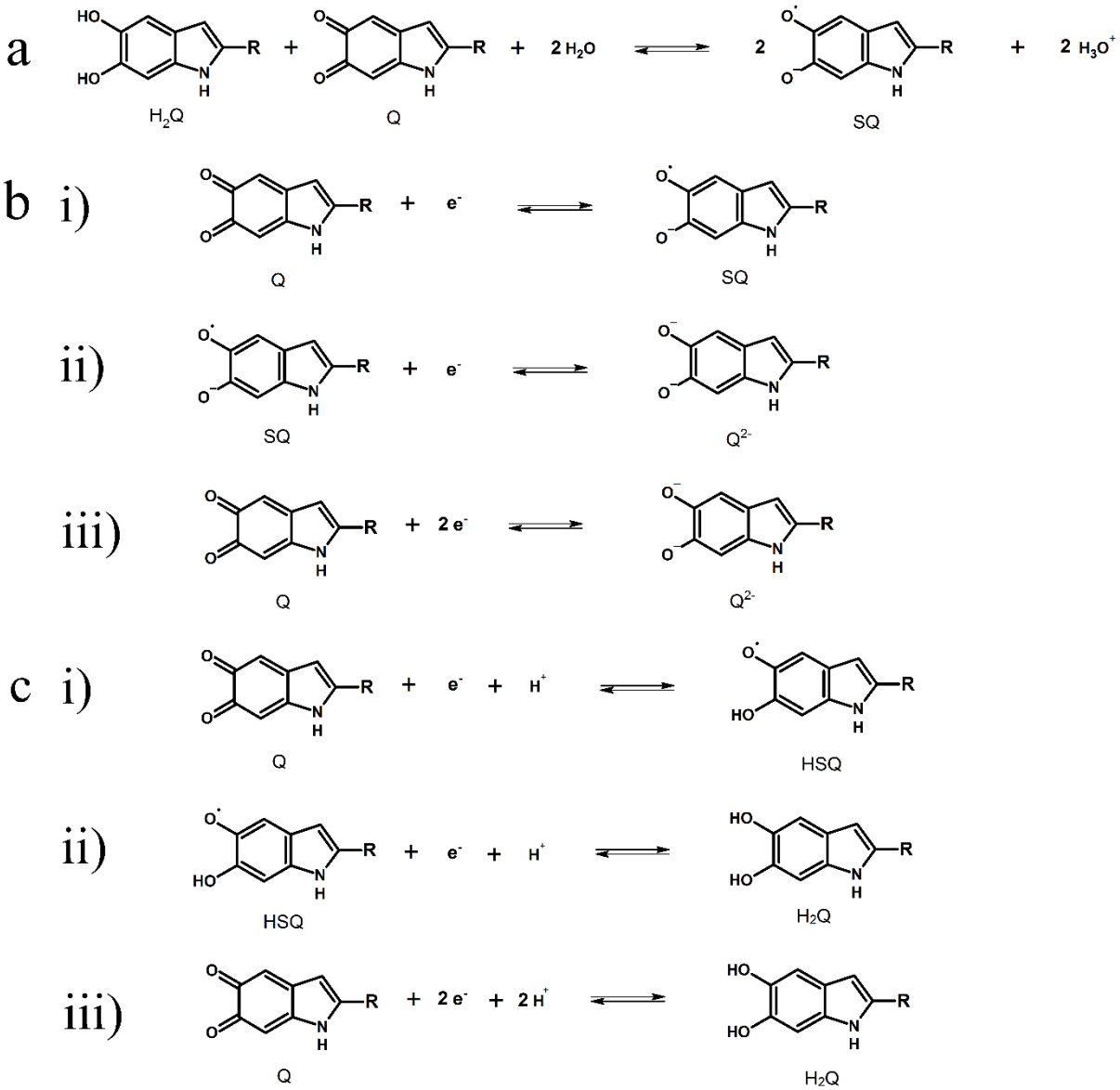

Figure 2: a) The overall comproportionation reaction. Moieties of two differing oxidative states (catechol and quinone) react together with water to form an intermediate oxidative state (the semiquinone) and hydronium. **b)**The reduction reactions used in the development of the model and used for equations 12 – 14. i) Reduction of the quinone to the semiquinone. ii) Reduction of the semiquinone to the deprotonated catechol. iii) Two electron reduction from the quinone to the deprotonated catechol. **c)** The reduction reactions depicted in b) above but with full protonation involved and used in equations 21 – 23. i) Reduction of the quinone to the protonated semiquinone/phenoxyl radical. ii) Reduction of the protonated semiquinone/phenoxyl radical to the catechol. iii) Two electron reduction from the quinone to the catechol.

A question may be raised regarding the potential deprotonation of the quinone itself. However, given the ease of tautomerisation (i.e. a large pool of reactant available) and subsequent deprotonation, it appears unlikely within the pH ranges discussed that the quinone itself undergoes deprotonation, and as such it will not be considered.

2.2. Basic Theory

The redox chemistry is modelled by accounting for 3 items: charge neutrality, mass or concentration balance and electron balance. The latter is particularly important since in redox chemistry the electron/oxidative state can change for a given monomer.[46] There are two major assumptions in the use of the equations below.

The charge balance equation utilized in the case of adding an acid is:

$$[H^+] - [OH^-] - [SQ] - [HQ^-] - 2[Q^{2-}] - [QM^-] - \frac{CV}{V+V_0} = 0 \qquad \text{(Eq. 1a)}$$

Where $[X]$ is the concentration of a particular species (see Figure 1 for quinone moiety labelling) and C is the concentration of the titrant solution. As will be seen in the discussion below, a comparison between DHI behavior will be made to published data on melanin by Chio *et al.* As such, the DHI solution will be modelled by the addition of 1M HCl.[47] V is the volume of titrant added and V_0 is the volume of the starting solution. For the addition of a base:

$$[H^+] - [OH^-] - [SQ] - [HQ^-] - 2[Q^{2-}] - [QM^-] + \frac{CV}{V+V_0} = 0 \qquad \text{(Eq. 1b)}$$

where the negative sign on the last term in Equation 1a is turned positive. We model a 1M NaOH solution addition in this case. For concentration balance, the total number of molecules (i.e. those with an indolequinone skeleton) must remain the same:

$$[H_2Q] + [HQ^-] + [Q^{2-}] + [HSQ] + [SQ] + [Q] + [HQM] + [QM^-] \ldots$$

$$-\frac{V_0([H_2Q]_0+[Q]_0)}{V+V_0}=0 \qquad \text{(Eq. 2)}$$

where $[H_2Q]_0$ and $[Q]_0$ are the idealized initial concentrations of catechol and quinone before any dissociations/reactions occur. Numerous models were run with varying starting fractions of $[H_2Q]_0$ to $[Q]_0$, i.e. at the start of a calculation it was assumed $[H_2Q]_0 + [Q]_0 = 100\%$ and the contribution from each monomer was varied. For more information, see supplementary information.

Finally, the electron balance is determined first by assuming that the semiquinone moieties are the baseline, zero oxidative state. Hence, the electron balance becomes:

$$[H_2Q] + [HQ^-] + [Q^{2-}] - [Q] - [HQM] + [QM^-] - \frac{V_0([H_2Q]_0-[Q]_0)}{V+V_0} = 0 \qquad \text{(Eq. 3)}$$

The variables in equations 1 to 3 can be related by a series of thermodynamic equilibrium constants as follows:

$$K_{a,H_2Q} = \frac{[HQ^-][H^+]}{[H_2Q]} \qquad \text{(Eq. 4)}$$

$$K_{a,HQ^-} = \frac{[Q^{2-}][H^+]}{[HQ^-]} \qquad \text{(Eq. 5)}$$

$$K_{a,HSQ} = \frac{[SQ][H^+]}{[HSQ]} \qquad \text{(Eq. 6)}$$

$$K_{a,HQM} = \frac{[QM^-][H^+]}{[HQM]} \qquad \text{(Eq. 7)}$$

$$K_{Q/HQM} = \frac{[Q]}{[HQM]} \qquad \text{(Eq. 8)}$$

$$E = E^o_{SQ/Q^{2-}} - \frac{RT}{F}\ln\frac{[Q^{2-}]}{[SQ]} \qquad \text{(Eq. 9)}$$

$$E = E^o_{Q/SQ} - \frac{RT}{F}\ln\frac{[SQ]}{[Q]} \qquad \text{(Eq. 10)}$$

$$K_w = [H^+][OH^-] = 10^{-14} \qquad \text{(Eq. 11)}$$

where equations 4 – 7 are acid dissociation constants for the various protonated entities (see Figure 1). Equation 8 is an equilibrium constant for the formation of the tautomer form for the quinone, i.e. quinone methide, which we will discuss in more detail in the results and discussion. Equations 9 – 10 are the one electron potentials for the redox reactions and equation 11 is accounting for water dissociation.

In the modelling, two models were tested. The first model assumed standard quinone/catechol behavior, i.e. omitting equations 7 & 8 and [HQM] & $[QM^-]$. The second model included everything. The equilibrium constants and reduction potentials were obtained from the literature or were estimated as below.

2.3. Estimating Standard One Electron Reduction Potentials: Assuming Standard Quinone Chemistry

Analytical equations exist for estimating the redox potentials for quinone/catechol systems,[48] [49] which are briefly covered here. Ideally, there are three redox reactions to describe quinone/catechol systems. They are:

$Q + e^- \rightleftarrows SQ$ (Eq. 12)

$SQ + e^- \rightleftarrows Q^{2-}$ (Eq. 13)

$Q + 2e^- \rightleftarrows Q^{2-}$ (Eq. 14)

where equations 12 & 13 are the one electron reductions and Equation 14 is the 2 electron reduction. Each of these reactions have their corresponding standard reduction potentials:

$$E^0_{Q/SQ} = \frac{RT}{F}\ln\frac{[SQ]}{[Q]} \quad \text{(Eq. 15)}$$

$$E^0_{SQ/Q^{2-}} = \frac{RT}{F}\ln\frac{[Q^{2-}]}{[SQ]} \quad \text{(Eq. 16)}$$

$$E^0_{Q/Q^{2-}} = \frac{RT}{2F}\ln\frac{[Q^{2-}]}{[Q]} \quad \text{(Eq. 17)}$$

where equations 15 & 16 are the equilibrium results for equations 9 & 10 and 17 is the equilibrium result for the 2 electron process. The apparent standard reduction potentials, though, can be changed as a function of pH, since each of the species involved have associated pK_as. Thus, at a particular pH, there are multiple versions of the same underlying species. Hence, pH dependent standard reduction potentials are determined for when the ratio of the concentrations of all oxidized species to concentrations of all reduced species is one. The resulting modified equations are:[48] [49]

$$E^{0,pH}_{Q/SQ} = E^0_{Q/SQ} - \frac{RT}{F}\ln K_{a,HSQ} + \frac{RT}{F}\ln\left(K_{a,HSQ} + [H^+]\right) \quad \text{(Eq. 18)}$$

$$E^{0,pH}_{SQ/Q^{2-}} = E^0_{SQ/Q^{2-}} - \frac{RT}{F}\ln\left(\frac{K_{a,H_2Q}K_{a,HQ^-}}{K_{a,HSQ}}\right) + \frac{RT}{F}\ln\left(\frac{K_{a,H_2Q}K_{a,HQ^-} + K_{a,H_2Q}[H^+] + [H^+]^2}{K_{a,HSQ} + [H^+]}\right) \quad \text{(Eq. 19)}$$

$$E^{0,pH}_{Q/Q^{2-}} = \frac{E^{0,pH}_{Q/SQ} + E^{0,pH}_{SQ/Q^{2-}}}{2} \quad \text{(Eq. 20)}$$

It should also be noted that the first two terms in the above equations 18 & 19 give you the effective reduction potentials for reactions 12 – 14 for fully protonated species:

$Q + e^- + H^+ \rightleftarrows HSQ$, $E^0_{Q/HSQ} = E^0_{Q/SQ} - \frac{RT}{F} \ln K_{a,HSQ}$ (Eq. 21)

$HSQ + e^- + H^+ \rightleftarrows H_2Q$, $E^0_{HSQ/H_2Q} = E^0_{SQ/Q^{2-}} - \frac{RT}{F} \ln \left(\frac{K_{a,H_2Q} K_{a,HQ^-}}{K_{a,HSQ}} \right)$ (Eq. 22)

$Q + 2e^- + 2H^+ \rightleftarrows H_2Q$, $E^0_{Q/H_2Q} = \frac{E^0_{Q/HSQ} + E^0_{HSQ/H_2Q}}{2}$ (Eq. 23)

Finally, the formation constant for the comproportionation reaction

$Q + Q^{2-} \rightleftarrows 2SQ^-$ (Eq. 24)

should also be considered:

$K_{comp} = \frac{[SQ]^2}{[Q][Q^{2-}]}$ (Eq. 25)

Similarly to the pH dependent reduction potentials, there will be a pH dependent apparent formation constant:

$K'_{comp,pH} = \frac{[SQ]^2_T}{[Q][Q^{2-}]_T}$ (Eq. 26)

where $[SQ]_T = [SQ] + [HSQ]$ and $\left[Q^{2-}\right]_T = [H_2Q] + [HQ^-] + \left[Q^{2-}\right]$. This apparent equilibrium constant is then related to Equation 25 by:

$K_{comp} = \frac{K_{a,HSQ}{}^2}{K_{a,H_2Q} K_{a,HQ^-}} \frac{\left(K_{a,H_2Q} K_{a,HQ^-} + K_{a,H_2Q} [H^+] + [H^+]^2 \right)}{\left(K_{a,HSQ} + [H^+] \right)^2} K'_{comp,pH}$ (Eq. 27)

The final relation is then:

$E^{0,pH}_{Q/SQ} - E^{0,pH}_{SQ/Q^{2-}} = \frac{RT}{F} \ln K'_{comp,pH}$ (Eq. 28)

Furthermore, an apparent comproportionation reaction constant can be estimated from the observations made on DHI-melanin systems by Szpoganicz *et al.*[45] These two variables are enough, coupled with previously reported pK_a's for DHI (see Table 1 & 2) and other literature results[51] [52] [53] to estimate the 1 electron reduction potentials of DHI as a function of H_2Q concentration. We note, though, that the estimation of an apparent comproportionation reaction constant derived from a complex polymer to infer the monomer properties naturally presents problems. The behavior of moieties in a complex polymer may only be loosely related to the corresponding monomer. However, given that melanin's properties, especially its free radical properties (see aforementioned EPR work in the introduction), can be well described by monomer like catechol/quinone chemistry it is a reasonable, if quite rough, initial starting point to use the results obtained for DHI-melanin and apply them to DHI. Naturally, the computational work presented here can certainly be

refined in the future once researchers obtain constants for DHI itself. For more detail, consult the supplementary information.

2.4. Estimating Standard One Electron Reduction Potentials: Accounting for Quinone Methide

DHI/DHI-melanin have an active quinone methide tautomer that can also protonate and deprotonate at moderate pH values.[45] [54] Hence, any modelling should account for tautomerisation. This will naturally impact the possible reduction potentials. However, in the entire derivation that follows, it assumes that the protonated quinone methide [HQM] can also be reduced since it is a similar molecule to the quinone, and as such could form a semiquinone like entity. However, the same cannot be said for the deprotonated state [QM^-], which has an additional charge on it and reduction would imply a doubly charged semiquinone. Given the above, equations 18 – 28 will have to be rewritten:

$$E_{Q/SQ}^{0,pH} = E_{Q/SQ}^{0} - \frac{RT}{F}\ln K_{a,HSQ} - \frac{RT}{F}\ln\left(1 + \frac{1}{K_{Q/HQM}}\right) + \frac{RT}{F}\ln\left(K_{a,HSQ} + [H^+]\right) \qquad \text{(Eq. 29)}$$

$$E_{SQ/Q^{2-}}^{0,pH} = E_{SQ/Q^{2-}}^{0} - \frac{RT}{F}\ln\left(\frac{K_{a,H_2Q}K_{a,HQ^-}}{K_{a,HSQ}}\right) + \frac{RT}{F}\ln\left(\frac{K_{a,H_2Q}K_{a,HQ^-} + K_{a,H_2Q}[\mathrm{H}^+] + [\mathrm{H}^+]^2}{K_{a,HSQ} + [\mathrm{H}^+]}\right) \qquad \text{(Eq. 30)}$$

Where the first three terms in equations 29 and the first two terms in equation 30 are the standard reduction potential for the fully protonated reduction reactions. Continuing:

$$K'_{comp,pH} = \frac{[\mathrm{SQ}]_T^2}{[Q]_T[\mathrm{Q}^{2-}]_T} \qquad \text{(Eq. 31)}$$

where $[\mathrm{SQ}]_T = [\mathrm{SQ}] + [\mathrm{HSQ}]$, $\left[\mathrm{Q}^{2-}\right]_T = [\mathrm{H_2Q}] + [\mathrm{HQ}^-] + \left[\mathrm{Q}^{2-}\right]$ and $[Q]_T = [\mathrm{Q}] + [\mathrm{HQM}]$.

Regarding the statement for $[Q]_T$, as mentioned above, one is assuming that the protonated quinone methide can also be reduced but not the deprotonated state.

Furthermore:

$$K_{comp} = K'_{comp,pH} \times \left(1 + \frac{1}{K_{\frac{Q}{HQM}}}\right)\left(\frac{K_{a,HSQ}{}^2}{K_{a,HQ^-}K_{a,H_2Q}}\right)\frac{\left([H+]^2 + K_{a,H_2Q}[H+] + K_{a,HQ^-}K_{a,H_2Q}\right)}{\left(K_{a,HSQ} + [H+]\right)^2} \qquad \text{(Eq. 32)}$$

As can be seen, equation 29 and 32 have been modified to include the tautomerisation constant $K_{Q/HQM}$. The estimation of $K_{Q/HQM}$ and the reduction potentials are presented in the supplementary information and the results are shown in Tables 1 & 2.

Molecular system	pK_{a,H_2Q}	pK_{a,HQ^-}	$pK_{a,HSQ}$	$pK_{a,HQM}$	$pK_{Q,HQM}$	pK_{comp}	$pK'_{comp,pH}$
DHI	**9.54(2)** [55] 9.59(2) [45]	**13.09(4)** [55] 12.1(1) [45]	**6.8(2)** [56]	-	-0.595 to 0.002[a]	-4.72 to -3.56 [a] -4.44 to -3.04 [d]	4.17 to 5.4[b] 4.35 to 5.75 [c]
DHICA	9.76(4) [55]	13.2(1) [55]	-	-	-	-	-
Dopamine	9.59(4) [55]	13.11(9) [55]	-	N/A	N/A	-	-
1,2 Catechol	9.24(6) [55] 9.45 [48]	13.0(1) [55] 12.8 [48]	5.0 [57]	N/A	N/A	-	-
DHI Melanin	9.44(3) [45]	10.56(5) [45]	-	**6.3 (3)** [45] [54]	-0.595 to 0.002[a]	-4.72 to -3.56 [a] -4.44 to -3.04 [d]	4.17 to 5.4[b] 4.35 to 5.75 [c]

[a] Estimated range determined from an initial H_2Q ($[H_2Q]_0$) fraction of 0.01 to 0.5. Also assumes Quinone Methide tautormerisation. See text for detail and supplementary information for more detail.

[b] Estimated range determined from an initial H_2Q ($[H_2Q]_0$) fraction of 0.01 to 0.5 at pH = 6.3. Also assumes Quinone Methide tautormerisation. See text for detail and supplementary information for more detail.

[c] Estimated range determined from an initial H_2Q ($[H_2Q]_0$) fraction of 0.01 to 0.5 at pH = 6.3. Also assumes no Quinone Methide tautomerisation. See text and supplementary information for more detail.

[d] Estimated range determined from an initial H_2Q ($[H_2Q]_0$) fraction of 0.01 to 0.5. Also assumes no Quinone Methide tautomerisation. See text and supplementary information for more detail.

Table 1: A table of equilibrium constant values for various related monomers to the building blocks of melanin. The values highlighted in bold indicate the values used in the modelling. The values underlined are the estimated values as explained in the theory and methods.

Molecular system	$E^o_{SQ/Q^{2-}}$ (V)	$E^o_{Q/SQ}$ (V)	$E^o_{Q/Q^{2-}}$ (V)	E^o_{HSQ/H_2Q} (V)	$E^o_{Q/HSQ}$ (V)	E^o_{Q/H_2Q} (V)	$E^{o,pH}_{Q/SQ}$ (V)	$E^{o,pH}_{SQ/Q^{2-}}$ (V)	$E^{o,\,pH}_{Q/Q^{2-}}$ (V)
DHI	-0.10 to -0.068 [a] -0.10 to -0.06 [d]	0.17 to 0.14 [a] 0.16 to 0.12 [d]	0.035 to 0.04[a] 0.03 [d]	0.83 to 0.87 [a] 0.84 to 0.88 [d]	0.57 to 0.53 [a] 0.56 to 0.52 [d]	**0.7 [50]**	-	-	-
DHICA	-	-	-	-	-	0.85 [50]	-	-	-
Dopamine	-	-	-	-	-	0.801 [59] 0.603 to 0.662 [60]	-	-	0.65 [61],[g]
1,2 Catechol	0.043 [48]	0.21 [f]	0.253 [f]	1.06 [f]	0.51 [f]	0.803 [62] 1.06 [48] 0.79 [f]	0.37 [57],[c]	0.21 [57],[c]	0.53 [57],[c]

DHI Melanin	-0.10 to -0.068 [b] -0.10 to -0.06 [e]	0.17 to 0.14 [b] 0.16 to 0.12 [e]	0.035 to 0.04[b] 0.03 [f]	0.83 to 0.87[b] 0.84 to 0.88[e]	0.57 to 0.53[b] 0.56 to 0.52 [e]	0.7 [e]	-	-	-

[a] Estimated range determined from an initial H_2Q ($[H_2Q]_0$) fraction of 0.01 to 0.5. Furthermore, it assumes that the K_{comp} and $pK'_{comp,pH}$ values determined for DHI-melanin are a fair estimation for the DHI monomer system. Also assumes Quinone Methide tautormerisation.
[b] Estimated range determined from an initial H_2Q ($[H_2Q]_0$) fraction of 0.01 to 0.5. Furthermore, it assumes that the pK_a's for DHI are a fair estimation for the polymer system. Also assumes Quinone Methide tautormerisation.
[c] For pH = 7.
[d] Estimated range determined from an initial H_2Q ($[H_2Q]_0$) fraction of 0.01 to 0.5. Furthermore, it assumes that the K_{comp} and $pK'_{comp,pH}$ values determined for DHI-melanin are a fair estimation for the monomer system. Also assumes no quinone methide tautomerisation.
[e] Estimated range determined from a H_2Q initial ($[H_2Q]_0$) fraction of 0.01 to 0.5. Furthermore, it assumes that the pK_a's for DHI are a fair estimation for the polymer system. Also assumes no quinone methide tautomerisation.
[f] Estimated using equations 18 to 20 and literature data.[48]
[g] For pH = 7.0 and corrected for Ag/AgCl electrode. Consult reference for additional pH dependence data points.

Table 2: A table of reduction potentials for various related monomers to the building blocks of melanin. All values quoted are vs SHE/NHE unless otherwise stated. The values highlighted in bold indicate the values used in the modelling. The values underlined are the estimated values as explained in the theory and methods.

What is interesting to observe is that, even accounting for tautomerisation, the standard reduction potentials are very similar to standard quinone/catechol behavior. Furthermore, even the potentials for the fully protonated systems are weakly affected. Hence, one should anticipate that if any difference will be observed in the free radical concentration behavior, it will be due to the relative amount of species due to the equilibrium constants, and not the reduction potentials.

2.5. Computational Method

At different pH levels the proportion of the above mentioned protonated and deprotonated redox reactions will differ. To capture this, the simplest method to determine the population of all the species at a given pH is to utilize the deprotonated 1 electron reduction in conjunction with the pK_a equations (at specific pH value) and perform an interactive non-linear regression calculation (see rest of theory section). This automatically will yield the overall reduction potential at that pH. The reason the protonated reduction equations do not have to be utilised is that these depend on pK_a parameters (e.g. equations 21 – 23), which are included in the iterative calculation elsewhere. As such, the only equations that are needed for a successful model are equations 1 – 6, 9 – 11 if one does not account for tautomerisation. If modelling the latter, equations 1 – 11 are needed.

Tables 1 & 2 shows the values for all constants used in the computational work (highlighted in bold) as derived from the literature.

For computational purposes, Equations 1 – 3 can be considered a set of algebraic equations $F_k(\boldsymbol{x}(V))$, where k is a balance equation, $\boldsymbol{x}$ is a vector $\boldsymbol{x}(V) = [x_1(V), x_2(V) \ldots x_n(V)]$ of basic variables $x_i(V)$ related to a particular variable V. For this work n = 3 and refers to the overall electrical potential E, the pH and the concentration of quinone [Q]. V will be the volume of a titrant added (HCl or NaOH). The aim is, at a particular value for V, to obtain the vector $\boldsymbol{x}(V)$ that solves the set of $F_k(\boldsymbol{x}(V)) = 0$ and zeroes the sum of the squares:

$$SS(V) = \sum_{k=1}^{n} (F_k(\boldsymbol{x}(V)))^2 = 0 \qquad \text{(Eq. 33)}$$

For this work, the above is determined via an iterative program using MATLAB based upon previously published work. [46] [63] Specifically, the optimset functionality was used within the fsolve function with an imbedded Levenberg-Marquardt least squares algorithm set to a termination tolerance of the function value of 10^{-10}.

3. Results and Discussion

3.1. DHI Redox Behavior

DHI's quinone counterpart is an *ortho*-quinone, and hence the initial inclination is to treat DHI and its various oxidative states according to well established models for such quinones.[48, 49] However, there is additional chemistry that needs to be accounted for, since DHI melanin systems exhibit a tautomerisation behavior via the formation of a quinone methide (HQM) (Figure 1),[45] which may have an impact on the various concentrations of various different species and in turn impact the redox chemistry. As such, two different models were employed as described in the methods section. The one treats DHI as a standard *ortho*-quinone system, and the other accounts for the formation of the quinone methide. The results are depicted in Figures 3 & 4.

Looking at Figure 3 first, we note that large changes in the behavior of all the chemical species occur around a pH of 9. This is clearly illustrated in part b, where there is a flattening of the potential, deviating away from the decreasing gradient around pH 9. The origin of the changes in the behavior is most likely due to the pK_a of the H_2Q, which starts at around 9.5 (see Table 1). The changes observed in parts 3a & 3b manifest themselves as a large increase in the total number of free radicals, as depicted in Figure 3c.

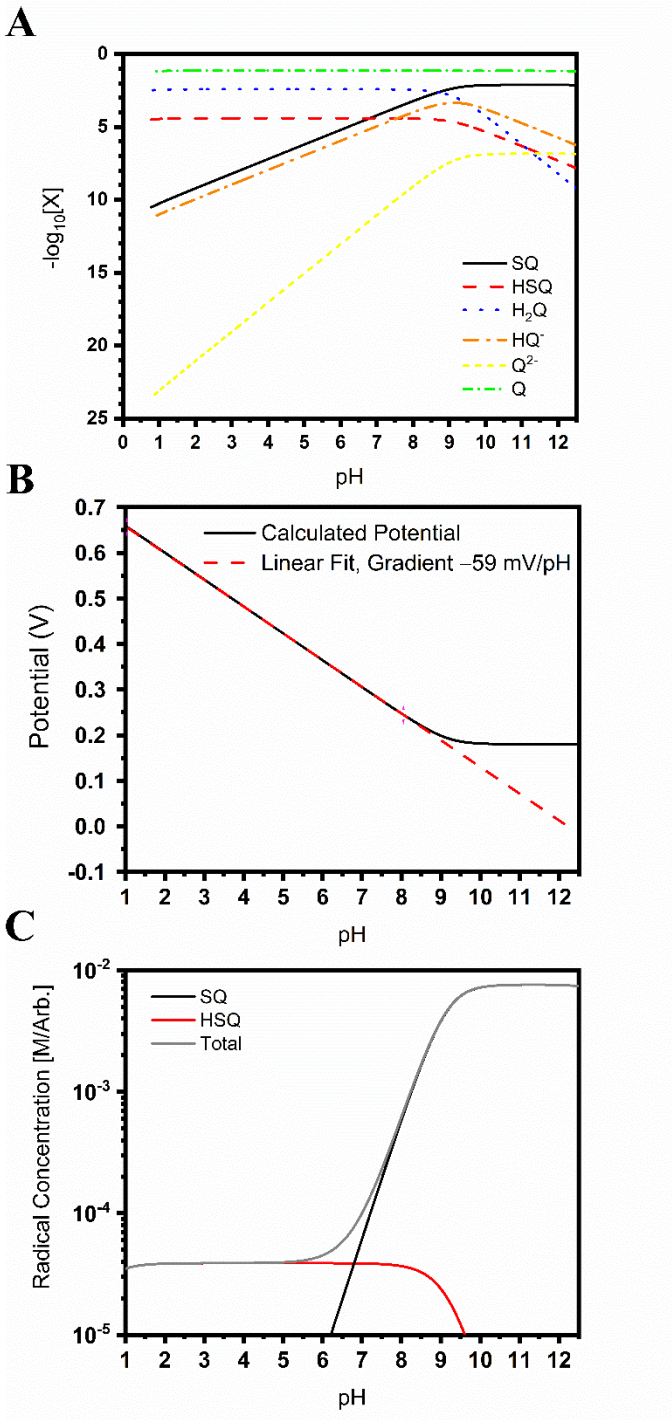

Figure 3: The results for modelling DHI according to the standard thermodynamic equations for an *ortho*-quinone. All data modelled to an initial H_2Q ($[H_2Q]_0$ fraction of 0.05. For different starting fractions ranging from 0.25 – 0.5, see Figures S8, which gave similar results. **A)** The concentration of different species as a function of pH. Note the $-\log_{10}$ scale for the concentration. The species labels are as taken from Figure 1. **B)** The calculated potential for the system as a function of pH. Depicted is the modelled gradient for the low to neutral pH behavior. **C)** The concentration of the radical species present as a function of pH, the protonated and deprotonated semiquinones. Also shown is the total curve.

Figure 4 provides an interesting contrast. Instead of clear changes at pH 9, changes in the gradients of the concentration of the species occur at around 7, associated with the HQM (see Table 1 pK_as). The equivalent changes that occur at pH 9 are much subdued in Figure 4 vis-à-vis Figure 3. This is further confirmed by

inspecting the potential in Figure 4b, which appears to maintain a relatively straight line across the entire pH range. The overall effect on the free radical content (SQ^- & HSQ) is to moderate the changes. The total free radical content is lowered by an order of magnitude at high pH with a clear indication of a potential decrease at very high pH. It is clear that when accounting for the quinone methide tautormerisation, the free radical content as well as the potential is heavily affected and that DHI should not be considered a simple, straightforward *ortho*-quinone system.

It is worth understanding the underlying reason for the behaviors observed in Figure 4, as it should give insight into more complex poly-indolequinone systems such as melanin and poly-dopamine. One would anticipate that when a semiquinone is being formed, that the reactant species, H_2Q (catechol) and Q (quinone), would be consumed at the same rate, i.e. the slopes at high pH should be parallel. However, this is clearly not the case. Instead, the slope for Q runs parallel to the HQM species. It is here that the origin of the suppression of the semiquinone production resides. Initially, Q and HQM are parallel, since the tautomerisation is pH independent. When the pK_a of HQM is reached, the quinone methide deprotonates. Naturally, this depletes the HQM pool. The HQM in turn is regenerated by depleting the quinone species, a reactant for semiquinone production. Essentially, there is additional competition for Q from HQM deprotonation, which make less Q available for semiquinones. Hence, the overall effect is to suppress the semiquinone concentration vis-à-vis a system which has no tautomer (Figure 3).

The potential vs pH curve in Figure 4b is also of interest. At low pH (1 – 6), the gradient is linear, and then there is a slight change lower with a similar gradient, but slightly offset. The overall gradient (-59 mV/pH) is close to a previously reported gradient by Horak and Weeks (-56 mV/pH between pH 1 – 10)[64] for DHI-melanin systems synthesized on electrodes, which gives further confidence in the model presented. What is of potential interest here is that such a high gradient should make DHI a material of interest for pH sensing, for the gradient is unusually high.[65]

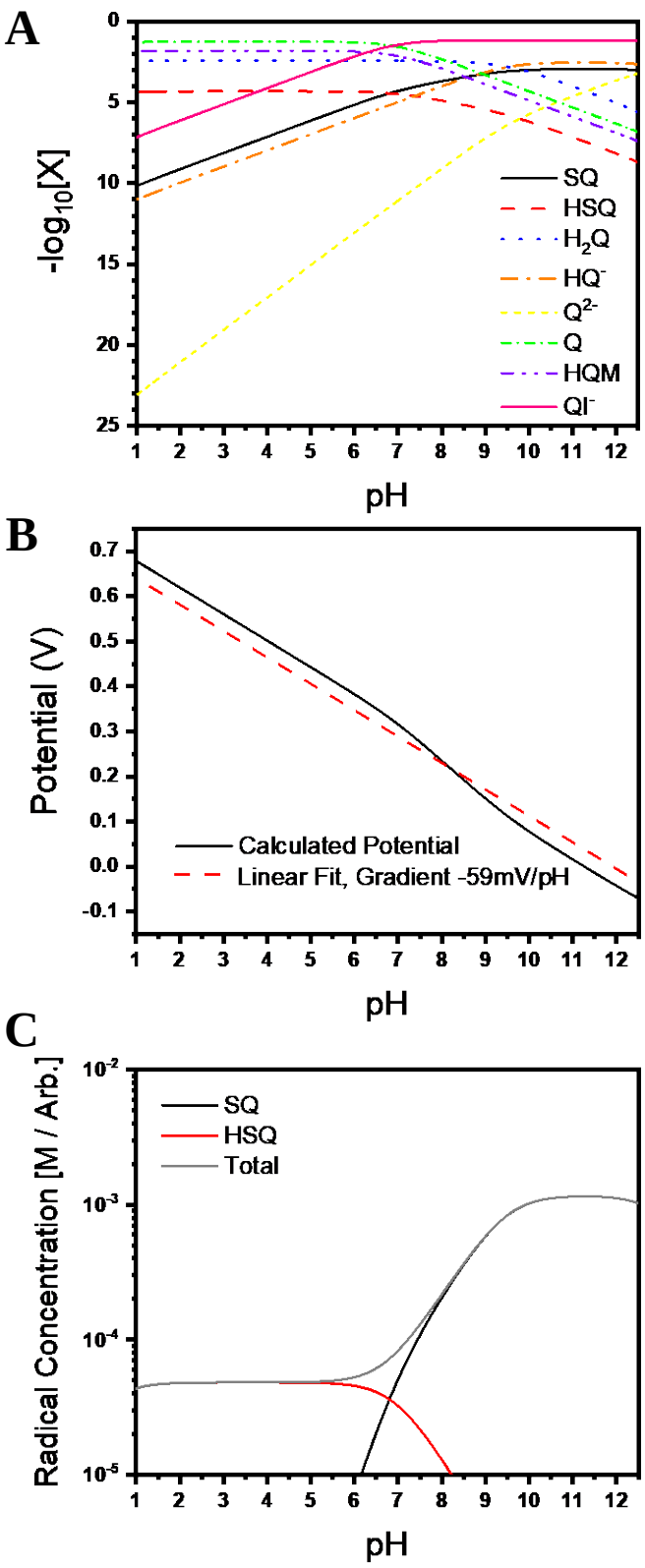

Figure 4: The results for modelling DHI accounting for quinone methide formation. All data modelled to an initial H_2Q ($[H_2Q]_0$) fraction of 0.05. For different starting fractions ranging from 0.25 – 0.5, see Figures S9, which gave similar results. **A)** The concentration of different species as a function of pH. Note the $-\log_{10}$ scale for the concentration. The species labels are as taken from Figure 1. **B)** The calculated potential for the system as a function of pH. Depicted is a modelled straight line gradient. **C)** The concentration of the radical species present as a function of pH, the protonated and deprotonated semiquinones. Also shown is the total curve.

3.2. Implications for more complex systems such as melanin and poly-dopamine

The key to the model as depicted in Figure 4 is the tautomerization constant used and deduced from Szpoganicz *et al.*[45] [54](see supplementary information), $K_{Q/HQM} = \frac{[Q]}{[HQM]} = 0.99 - 3.9$. The model indicates that there is a significant fraction of quinone methide in a potential DHI solution, which is at least consistent with the data from Szpoganicz *et al.* The deduction of the DHI quinone methide pK_a was obtained on model DHI compounds, in which a DHI molecule was methylated and allowed to polymerise and compared to non-methylated DHI polymers, while observing the effects of buffering in a titration experiment. Since a derived experimental result used in the above model is based on a more complex system, a system that is closer to a poly-dopamine or a melanin system, it is useful to investigate the applicability of the above modelling of DHI to these latter systems.

It is believed that the effect of the tautomerisation of DHI moieties (and by extension, potentially DHICA moieties) in melanin may indeed manifest itself in published electron paramagnetic resonance (EPR) data on melanin solutions. As noted in the introduction, melanin is a disordered oligomeric system derived from DHI and DHICA, with many of these moieties present on the surface of melanin particles. Hence, we should anticipate much of the redox chemistry explored above to be relevant to the melanin systems since melanin particle surfaces are redox active. [51] [66] The best experimental EPR work on melanin solutions is by Chio *et al.*,[47, 67] (Figure 5). Chio *et al.*'s data is attractive in that it is quantitative. Furthermore, EPR is an attractive data set to look at since free radicals by their nature are redox active species in the melanins.

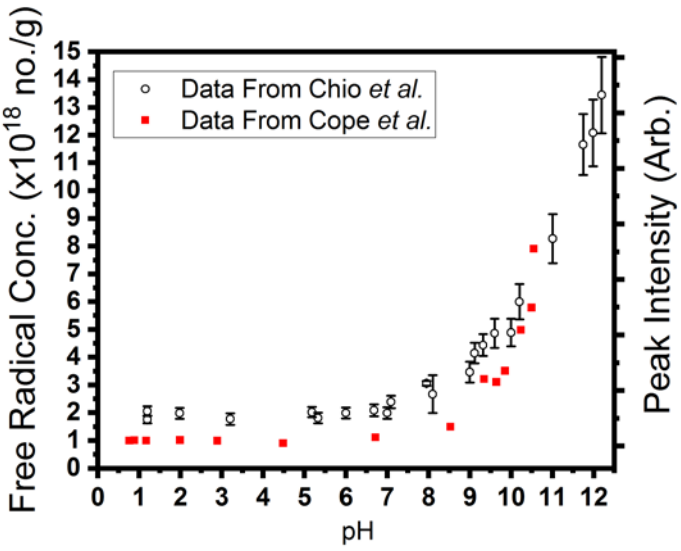

Figure 5: The pH/free radical concentration data as reported by Chio *et al.*[47] Shown as well is work published by Cope *et al.*[68]. However, these latter authors only reported the peak height intensity on an arbitrary scale, and hence their data is not as useful as Chio *et al.*'s data. Though, it is clear that the two data sets are qualitatively similar.

If one assumed the initial mass concentrations as reported by Chio *et al.*[47] and a 90/10 mixture of DHI/DHICA (to account for COOH content as expected for synthetic melanins),[14] an initial concentration of $[H_2Q]_0 + [Q]_0 = 0.077$ M is obtained. One can then obtain a total free radical concentration using the modelling in Figure 3c & 4c and overlay it on the data in Figure 5 to obtain Figure 6.

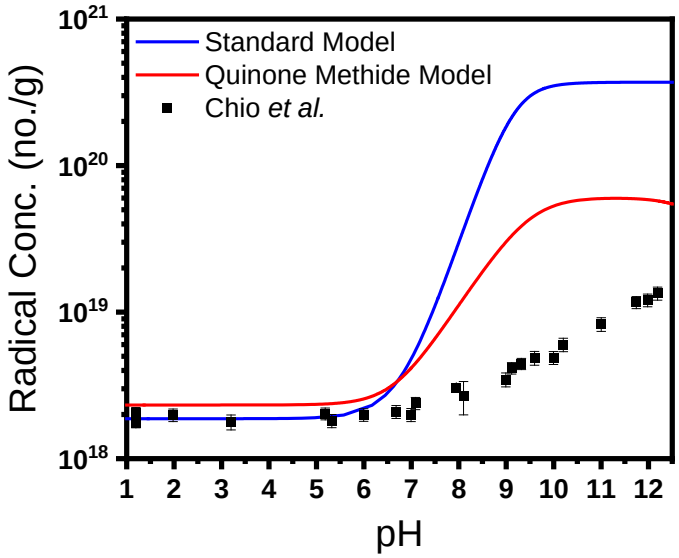

Figure 6: Presented is the modelling of DHI solutions and the expected radical concentration as a function of pH and comparing them to the published data by Chio *et al*. The blue line assumes a standard quinone system (Standard model, i.e. Figure 3 results) and the red line assumes a system accounting for the quinone methide (due to tautomerisation, i.e. Figure 4 results). Both models assumed a starting monomer fraction of 0.05 for H_2Q ($[H_2Q]_0$).

The first observation is to note that the essential qualitative behavior is correctly captured, i.e. at low pH, the radical concentration is constant but it then increases at high pH. However, as can be clearly seen, there are differences at high pH. From modelling done on other quinone systems, the increase in semiquinone concentration at high pH tends to be many orders of magnitude,[62] i.e. Figure 3, and is represented by the blue curve. Yet, melanin is quite different in that the increase is barely 1 order of magnitude. Looking at Figure 6, it is clear that the red data curve (using Figure 4 modelling) is a better approximation as it decreases the gap between model and data by about 1 order of magnitude. Hence, it is clear that tautomerization of the quinone and deprotonation of the quinone methide is a major correction to help explain the data. In light of the above, the rest of the discussion will follow the modelling that includes the full quinone methide behavior.

There is an additional point that needs to be covered. In Chio *et al.*'s observations, they measured the linewidth of their EPR signals and found that it changed dramatically at around pH~6. Concomitantly, there was a change in the isotropic g value of the species from ~2.0034 to ~2.0043 with increasing pH, with an inflection point around pH~7. What the modelling in Figure 4 & 6 may be indicating is that what Chio *et al.*[47] were observing was the deprotonation of semiquinones with increasing pH. This is similar to the observations made[69] [70] in which a line shape analysis showed that there was a pH dependence on the linewidth. It has been proposed over the years that there are at least two radical species in melanin,[25] [26] [22] [28] [27] [69] [70] [71] [72] [18] with various candidates being proposed along the way. Recent work on solid state melanin has suggested that the two species may be a carbon centered radical (g = 2.0033, inference was based purely upon the g value) and the other the semiquinone radical (2.0045).[25] [22] Figure 6 may suggest that the identity of the carbon centered radical may be a protonated semiquinone. This is similar to suggestions made by Chio *et al.*[47] and others. [69] However, it has been noted that other species may be present,[69] [26] [27] and given some stark differences in behavior between solid and solution state measurements[25] (as well as computational results[26]) it may be that there is another free radical species of order 10^{18} spins/gram that may be present alongside the semiquinones.

The data as presented in Figure 6 also has implications for understanding charge transport of the melanins and the poly-dopamine systems. It has been demonstrated elsewhere that the semiquinone free radical is a marker for the hydration dependent conductivity of melanin in the solid state.[28] The main idea is that, as melanin is hydrated, the comproportionation reaction shifts from quinone and catechol to the production of semiquinone radicals and hydronium (Figure 2a). However, the data presented in Figures 4 & 6 models both the comproportionation reaction and also semiquinone deprotonation, similarly as for other quinone systems.[62] [73] Clearly, the comproportionation reaction is insufficient on its own. As a result, the current hydration dependent charge transport model[24] that to date has relied on qualitative arguments based upon the comproportionation reaction for understanding[24] [22] [28] [29] needs to be updated to account for semiquinone deprotonation.

However, some additional insight on the comproportionation reaction can be obtained for melanin systems based upon the DHI chemistry explored above. In previous work by Motovilov *et al.*[29], the Gibbs free energy of reaction for the comproportionation reaction in melanin was estimated to be around 1.08 eV. The

calculation was based upon 1,2 benzoquinone redox potentials and appeared to give a result in good agreement with the experimental results obtained upon melanin. It suggested that single molecule moieties may give a good starting point in understanding these complex polymeric system. However, the estimations were done in the absence of accounting for the effects of pH on the redox potentials and didn't account for the potential effects of quinone methide tautomerisation and deprotonation. Hence, a new estimation should be given with the benefit of the model as presented in Figure 4 above, since it is also specifically based upon DHI information, which is more pertinent to the melanin systems. If one reconsiders the work of Motovilov *et al*.[29], the apparent equilibrium constant they used can be rewritten as

$$K_M = K_{a,H_2Q} K_{a,HQ^-} K_{comp} = e^{-\frac{\Delta G}{RT}}$$

where K_{comp} is found in equation 32 above and ΔG reflects the Gibbs free energy of reaction. Given that a range of 3.8×10^3 to 50×10^3 for K_{comp} has been determined, it translates into a ΔG range of 1.12 eV to 1.06 eV. Given the experimental results of Motovilov *et al*. yielding a value of 1.08 eV, the model result is well within their data.

3.3. DHI redox chemistry: An explanation for free radical behavior in complex systems?

Figure 4 & 6 assumed that there is a 5% catechol population (H_2Q), in line with previously published literature[52] (see also supplementary information). Naturally, since melanin is a disordered material, 5% may not always be true. Moreover, since melanin is formed under oxidative conditions[47] [12] [14] [9], one could anticipate an even higher content for quinone formation vis-à-vis catechol. Variation in such initial concentrations may also explain the differences between the model and a more complex system as seen in Figure 6. Thus, the effect of different starting H_2Q content is explored in Figure 7, where the initial H_2Q starting fraction is varied between 1 –25%.

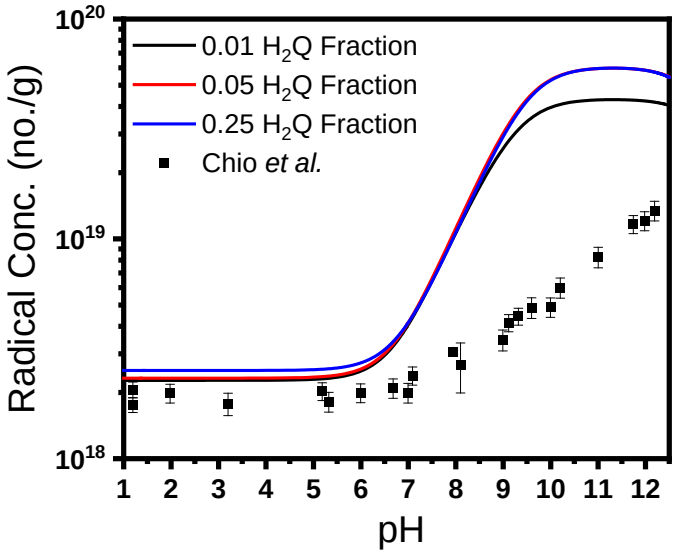

Figure 7: Presented is the modelling of the radical concentration (assuming different initial total fraction of H_2Q moieties ($[H_2Q]_0$), see legend) and the data as published by Chio *et al.* It can be seen that lowering the H_2Q concentration does decrease the total semiquinone production, with the trend being non-linear.

Figure 7 shows that lowering the concentration of the initial H_2Q fraction leads to a lowering of the total semiquinone production at high pH, but not necessarily at low pH. Furthermore, the trend is not linear, and it is clearly not enough to account for the discrepancy between the data and the model. It should be clear that the initial starting concentration can be lowered even further, but the question then arises as to whether such low fractions (<1% H_2Q) are representative for melanin or poly-dopamine systems. Hence, initial concentrations do not appear to explain the differences seen in Figure 6.

A key issue is that the DHI curves as presented in Figures 4 – 7 are probably the best that can be achieved in light of all the literature results presented above, while allowing only 3 fitting parameters and assuming that DHI is directly applicable to melanin. The model, though, is out by a factor of 3 at peak semiquinone concentration vs. the data. Nonetheless, to see whether the DHI model can be optimized to the melanin data and to test the model sensitivity, the pK_as of the various acidic groups were varied. The results are shown in Figure 8. The first model (red line) assumes the extremes in the literature values of the pK_as, i.e. using the values at the extremes of the reported uncertainties. As can be seen, this does not have a significant impact. However, the second model, which is similar to Figures 4 – 7 but changing the pK_a of the protonated semiquinone to 7.5, dramatically decreases the semiquinone peak (parameters used for the models in Figures 5 – 8 are given in Table 3). What this indicates is that if "wiggle room" in the values of all the pK_as are

allowed, the published data can be more easily simulated. Furthermore, this potential variation in the pK_as will require the deprotonation of all species to shift higher to some extent. However, at such a point we would be moving away from the monomer DHI system, and may indeed be moving closer to the average pK_as present within a polymeric system such as melanin or poly-dopamine. The values of such thermodynamic variables needs more careful investigation in the future to substantiate the above considerations.

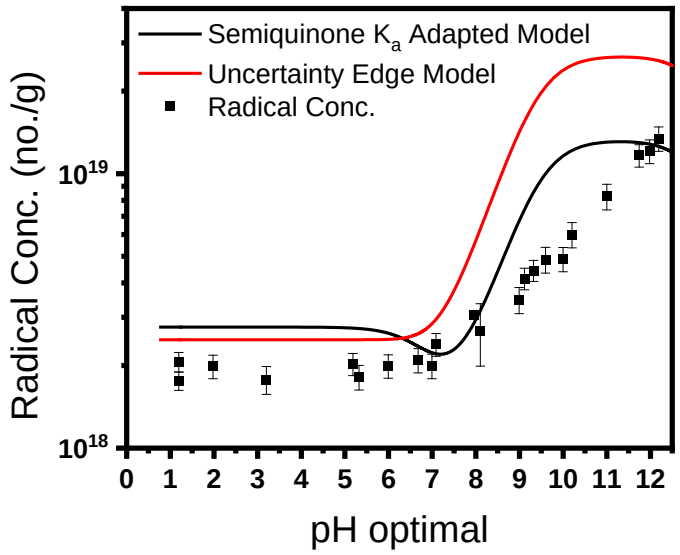

Figure 8: Optimised models vs published data of Chio *et al.* The data referred to as the uncertainty edge is predicated on values for the pK_as at the extremities of their reported uncertainty (see Table 1). The semiquinone K_a adapted model refers to modification of the pK_as of the semiquinone protonation and quinone methide protonation. The values that were estimated and used can be seen in table 3.

In short, it is easy to imagine that slight changes in the pK_as as well as the redox potentials should be able to account for the differences seen between the monomer models and the complex polymer data.

Model	pK_{a,H_2Q}	pK_{a,HQ^-}	$pK_{a,HSQ}$	$pK_{a,HQM}$	$pK_{Q,HQM}$	pK_{comp}	$E^0_{SQ/Q^{2-}}$ **(V)**	$E^0_{Q/SQ}$ **(V)**	$\frac{[H_2Q]_0}{C}$
Figures 7	9.54	13.09	6.8	6.3	-0.595	-4.17	-0.104	0.175	0.01
Figure 8, Red Data	9.56	13.13	7.0	6	-0.60	-4.46	-0.0981	0.165	0.01
Figure 8, Black Data	9.54	13.09	7.4	6	-0.60	-3.69	-0.074	0.144	0.01

Table 3: The constants used in the final models depicted in Figure 8.

Finally, a question can be raised in regards to the model. It is easy to include COOH deprotonation behavior into the DHI model to see if a DHI/DHICA mixture could potentially change the pH dependent behavior, and hence give potential insight into melanin behavior. However, after creating such a model, no difference in the models could be observed on any of the metrics, including the overall potential. The semiquinone formation appears to be independent of the behavior of the COOH groups. This leads to two additional points.

The first is that the published melanin data should then be replicable using a poly-dopamine system. After all, to first order, poly-dopamine can be thought of as a melanin without the COOH groups, i.e. a poly DHI system. Thus, all the modelling above (including constant estimations) and the conclusions drawn should be applicable to poly-dopamine.

The second point is that the model may not be completely transferred onto a solid-state melanin system to probe questions about conductivity. In the solid-state experiments, in which water content is increased, the first order expectation is to get ionization due to dilution, which will lead to proton conductivity. However, as recently suggested[29], the protons from the COOH may only be a minor component of the solid-state proton conductivity. In short, it remains to be seen whether the above model can actually be transferred over to a solid-state situation.

Overall, it does appear that monomeric DHI behavior is a good first step to explain the gross features of more complex poly-indolequinone systems, but certainly not the finer details. The origins of such discrepancies are numerous, but a likely candidate is related to the morphology of the underlying oligomeric stacking of the materials such as melanin. Different ratios of DHI and DHICA are known to change the morphology and hence lead to differences in the observed EPR spectra[74], implying some differences in the underlying redox chemistry.

3.4. Future Work

The above modelling of DHI does capture many of the key features of more complex systems, and has delivered new insight that thus far has never been suggested in the literature. However, the DHI models themselves should be considered a work in progress, never mind models to capture the behavior of more complex systems. Hence, there is a veritable list of questions to be answered experimentally such as:

1. What are the experimental 1 electron reduction potentials for DHI in the quinone/semiquinone and semiquinone/catechol reactions?
2. What is the experimental tautomerisation equilibrium constant for the quinone methide formation for molecular DHI?
3. What is the acid dissociation constant for molecular DHI quinone methide in solution?
4. What are the corresponding values for DHICA and dopamine?
5. Can one obtain apparent dissociation constants (including the semiquinone dissociation) and reduction potentials for poly-dopamine, DHI-melanin and melanin proper (and its various DHI/DHICA ratios)?
6. Furthermore, and more challenging, can one obtain activity constants for each of the above systems?

In addition to the above questions, supplementary questions and ways to test the veracity of the models presented here can be added. For example, if the model presented here can be applied to poly-dopamine, then a replication of the methods of Chio *et al.* on solution poly-dopamine should yield similar results. In addition, if the quinone methide is responsible for the suppression of the semiquinone production, then doing a pH dependent EPR experiment on N-methylated DHI should stop the quinone methide tautomerisation (as seen by Szpoganicz *et al.*[45]) and lead to a greater semiquinone content at high pH. Also, if a method can be devised to enhance the catechol content of the melanin/DHI/poly-dopamine, then the increase in H_2Q content should lead to a greater semiquinone content. Finally, potential vs pH curves should be obtained alongside any EPR/pH data to confirm the basic behavior of the models.

Looking further afield, the model presented here can form the basis for understanding DHI/poly-dopamine/melanin interactions with metal ions, similarly as was done by Szpoganicz *et al.*[45] However, with a greater understanding as presented here, the potential redox reactions with metal ions can also be predicted. Finally, the models should form the basis for understanding the solid state, especially pertinent to the melanin on which there is systematic hydration dependent conductivity. If adapted for hydration dependent behaviour, it may be able to predict what the conductivity behaviour of melanin (and by extension poly-dopamine) should be and give insight in potential synthetic strategies for enhancing the conductive properties of the poly-indolequinone polymers.

4. Conclusions

In conclusion, a model has been presented to holistically explain the free radical/redox chemistry for dihydroxyindole. The models indicate the significant role the quinone methide tautomerisation play in the redox properties of dihydroxyindole, which thus far has not been reported. Furthermore, estimations for various equilibrium constants and reduction potentials are presented. Finally, the redox models presented here have explanatory power for more complex poly-indolequinone systems.

Supporting Information

The Supporting Information is available free of charge at DOI: XXXXXXXX.

Supporting Figures S1 − S9, Equations S1 – 12, text and references S1 – S4.

Acknowledgements

A.B.M. is a Sêr Cymru II fellow and the results incorporated in this work have received funding from the European Union's Horizon 2020 research and innovation program under the Marie Skłodowska-Curie grant agreement No 663830. Also thanks is given to Dr. Hamish Cavaye and Dr. Kostya Motovilov for their suggestions.

References

[1] N. Amdursky, E.D. Glowacki, P. Meredith, Macroscale Biomolecular Electronics and Ionics, Advanced Materials 31 (2019) 1802221.
[2] Y. Liu, K. Ai, L. Lu, Polydopamine and Its Derivative Materials: Synthesis and Promising Applications in Energy, Environmental, and Biomedical Fields, Chemical Reviews 114 (2014) 5057-5115.
[3] P. Meredith, C.J. Bettinger, M. Irimia-Vladu, A.B. Mostert, P.E. Schwenn, Electronic and optoelectronic materials and devices inspired by nature, Reports on Progress in Physics 76 (2013) 034501.
[4] H. Lee, S.M. Dellatore, W.M. Miller, P.B. Messersmith, Mussel-inspired surface chemistry for multifunctional coatings, Science 318 (2007) 426-430.
[5] H. Lee, B.P. Lee, P.B. Messersmith, A reversible wet/dry adhesive inspired by mussels and geckos, Nature 448 (2007) 338-342.
[6] J. Bothma, J. de Boor, U. Divakar, P. Schwenn, P. Meredith, Device-quality electrically conducting melanin thin films., Advanced Materials 20 (2008) 3539-3542.
[7] S.N. Dezidério, C.A. Brunello, M.I.N. da Silva, M.A. Cotta, C.F.O. Graeff, Thin films of synthetic melanin, Journal of Non-Crystalline Solids 338-340 (2004) 634-638.
[8] J. Wünsche, F. Cicoira, C.F.O. Graeff, C. Santato, Eumelanin thin films: solution-processing, growth, and charge transport properties, Journal of Materials Chemistry B 1 (2013) 3836-3842.
[9] M. d'Ischia, A. Napolitano, V. Ball, C.T. Chen, M.J. Buehler, Polydopamine and Eumelanin: From Structure−Property Relationships to a Unified Tailoring Strategy, Accounts of Chemical Research 47 (2014) 3541-3550.
[10] A.B. Mostert, K.J.P. Davy, J.L. Ruggles, B.J. Powell, I.R. Gentle, P. Meredith, Gaseous adsorption in melanins: Hydrophilic biomacromolecules with high electrical conductivities, Langmuir 26 (2010) 412-416.
[11] A.J. Clulow, A.B. Mostert, M. Sheliakina, A. Nelson, N. Booth, P.L. Burn, I.R. Gentle, P. Meredith, The structural impact of water sorption on device-quality melanin thin films, Soft Matter 13 (2017) 3954-3965.
[12] P. Meredith, T. Sarna, The physical and chemical properties of eumelanin, Pigment Cell Research 19 (2006) 572-594.
[13] S. Ito, A chemist's view of melanogenesis, Pigment Cell Research 16 (2003) 230-236.

[14] M. d'Ischia, K. Wakamatsu, A. Napolitano, S. Briganti, J.C. Garcia-Borron, D. Kovacs, P. Meredith, A. Pezzella, M. Picardo, T. Sarna, J.D. Simon, S. Ito, Melanins and melanogenesis: methods, standards, protocols, Pigment Cell Research 26 (2013) 616-633.
[15] V. Gray-Schopfer, C. Wellbrock, R. Marais, Melanoma biology and new targeted therapy, Nature 445 (2007) 851-857.
[16] F.A. Zucca, G. Giaveri, M. Gallorini, A. Albertini, M. Toscani, G. Pezzoli, R. Lucius, H. Wilms, D. Sulzer, S. Ito, K. Wakamatsu, L. Zecca, The Neuromelanin of Human Substantia Nigra: Physiological and Pathogenic Aspects, Pigment Cell Research 17 (2004) 610-617.
[17] W.D. Bush, J. Garguilo, F.A. Zucca, A. Albertini, L. Zecca, G.S. Edwards, R.J. Nemanich, J.D. Simon, The surface oxidation potential of human neuromelanin reveals a spherical architecture with a pheomelanin core and a eumelanin surface, Proceeds of the National Academy of Science USA 103 (2006) 14785-14789.
[18] T. Sarna, ProDerties and function of the ocular melanin - A photobiophysical view, Journal of Photochemistry and Photobiology B: Biology 12 (1992) 215-258.
[19] P. Meredith, B.J. Powell, J. Riesz, S.P. Nighswander-Rempel, M.R. Pederson, E.G. Moore, Towards structure–property–function relationships for eumelanin, Soft Matter 2 (2006) 37-44.
[20] E. Dadachova, R.A. Bryan, X. Huang, T. Moadel, A.D. Schweitzer, P. Aisen, J.D. Nosanchuk, A. Casadevall, Ionizing Radiation Changes the Electronic Properties of Melanin and Enhances the Growth of Melanized Fungi, PLoS ONE 2 (2007) e457.
[21] J. Riesz, J. Gilmore, P. Meredith, Quantitative photoluminescence of broad band absorbing melanins: a procedure to correct for inner filter and re-absorption effects, Spectrochimica acta. Part A 61 (2005) 2153-2160.
[22] S.B. Rienecker, A.B. Mostert, G. Schenk, G.R. Hanson, P. Meredith, Heavy water as a probe of the free radical nature and electrical conductivity of melanin, Journal of Physical Chemistry B 119 (2015) 14994-15000.
[23] M.R. Powell, B. Rosenberg, The Nature of the Charge Carriers in Solvated Biomacromolecules, Bioenergetics 1 (1970) 493-509.
[24] A.B. Mostert, B.J. Powell, F.L. Pratt, G.R. Hanson, T. Sarna, I.R. Gentle, P. Meredith, Role of semiconductivity and ion transport in the electrical conduction of melanin, Proceedings of the National Academy of Sciences USA 109 (2012) 8943-8947.
[25] A.B. Mostert, G.R. Hanson, T. Sarna, I.R. Gentle, B.J. Powell, P. Meredith, Hydration-Controlled X-Band EPR Spectroscopy: A Tool for Unravelling the Complexities of the Solid-State Free Radical in Eumelanin, Journal of Physical Chemistry B 117 (2013) 4965-4972.
[26] A. Batagin-Neto, E.S. Bronze-Uhle, C.F.O. Graeff, Electronic structure calculations of ESR parameters of melanin units, Phys. Chem. Chem. Phys. 17 (2015) 7264-7274.
[27] J.V. Paulin, A. Batagin-Neto, C.F.O. Graeff, Identification of Common Resonant Lines in the EPR Spectra of Melanins, Journal of Physical Chemistry B 123 (2019) 1248-1255.
[28] A.B. Mostert, S.B. Rienecker, C. Noble, G.R. Hanson, P. Meredith, The photoreactive free radical in eumelanin, Science Advances 4 (2018) eaaq1293.
[29] K.A. Motovilov, V. Grinenko, M. Savinov, Z.V. Gagkaeva, L.S. Kadyrov, A.A. Pronin, Z.V. Bedran, E.S. Zhukova, A.B. Mostert, B.P. Gorshunov, Redox chemistry in the pigment eumelanin as a function of temperature using broadband dielectric spectroscopy, RSC Advances 9 (2019) 3857-3867.
[30] M. Sheliakina, A.B. Mostert, P. Meredith, Decoupling Ionic and Electronic Currents in Melanin, Advanced Functional Materials 28 (2018) 1805514.
[31] A.B. Mostert, B.J. Powell, I.R. Gentle, P. Meredith, On the origin of electrical conductivity in the bio-electronic material melanin, Applied Physics Letters 100 (2012) 093701.
[32] A.B. Mostert, S. Rienecker, M. Sheliakina, P. Zierep, G.R. Hanson, J.R. Harmer, G. Schenk, P. Meredith, Engineering Proton Conductivity in Melanin Using Metal Doping, Journal of Materials Chemistry B (2020).
[33] M. Reali, A. Gouda, J. Bellemare, D. Ménard, J.-M. Nunzi, F. Soavi, C. Santato, Electronic Transport in the Biopigment Sepia Melanin, ACS Applied Bio Materials 3 (2020) 5244-5252.
[34] M. Sheliakina, A.B. Mostert, P. Meredith, An All-Solid-State Biocompatible Ion-to-Electron Transducer for Bioelectronics, Material Horizons 5 (2018) 256-263.
[35] M.P. da Silva, J.C. Fernandes, N.B. de Figueredo, M. Mulato, C.F.O. Graeff, Melanin as an active layer in biosensors, AIP Advances 4 (2014) 037120.
[36] M. Ambrico, P.F. Ambrico, A. Cardone, T. Ligonzo, S.R. Cicco, R. Di Mundo, V. Augelli, G.M. Farinola, Melanin Layer on Silicon: an Attractive Structure for a Possible Exploitation in Bio-Polymer Based Metal-Insulator-Silicon Devices, Advanced Materials 23 (2011) 3332.
[37] L. Migliaccio, M. Gryszel, V. Đerek, A. Pezzella, E.D. Głowacki, Aqueous photo(electro)catalysis with eumelanin thin films, Material Horizons 5 (2018) 984-990.
[38] P. Kumar, E. Di Mauro, S. Zhang, A. Pezzella, F. Soavi, C. Santato, F. Cicoira, Melanin-based flexible supercapacitors, Journal of Materials Chemistry C 4 (2016) 9516-9525.
[39] J. Wünsche, Y. Deng, P. Kumar, E. Di Mauro, E. Josberger, J. Sayago, A. Pezzella, F. Soavi, F. Cicoira, M. Rolandi, C. Santanto, Protonic and Electronic Transport in Hydrated Thin Films of the Pigment Eumelanin, Chemistry of Materials 27 (2015) 436-442.

[40] M. Sugumaran, J. Evans, S. Ito, K. Wakamatsu, Nonenzymatic Spontaneous Oxidative Transformation of 5,6-Dihydroxyindole, International Journal of Molecular Sciences 21 (2020) 7321.
[41] S. Ito, M. Sugumaran, K. Wakamatsu, Chemical Reactivities of ortho-Quinones Produced in Living Organisms: Fate of Quinonoid Products Formed by Tyrosinase and Phenoloxidase Action on Phenols and Catechols, International Journal of Molecular Sciences 21 (2020) 6080.
[42] M. Sugumaran, Reactivities of Quinone Methides versus o-Quinones in Catecholamine Metabolism and Eumelanin Biosynthesis, International Journal of Molecular Sciences 17 (2016) 1576.
[43] Y.V. Il'ichev, J.D. Simon, Building Blocks of Eumelanin: Relative Stability and Excitation Energies of Tautomers of 5,6-Dihydroxyindole and 5,6-Indolequinone, Journal of Physical Chemistry B 107 (2003) 7162-7171.
[44] A. Pezzella, O. Crescenzi, A. Natangelo, L. Panzella, A. Napolitano, S. Navaratnam, R. Edge, E.J. Land, V. Barone, M. d'Ischia, Chemical, Pulse Radiolysis and Density Functional Studies of a New, Labile 5,6-Indolequinone and Its Semiquinone, The Journal of Organic Chemistry 72 (2007) 1595-1603.
[45] B. Szpoganicz, S. Gidanian, P. Kong, P. Farmer, Metal binding by melanins: studies of colloidal dihydroxyindole-melanin, and its complexation by Cu(II) and Zn(II) ions, Journal of Inorganic Biochemistry 89 (2002) 45-53.
[46] T. Michałowski, M. Toporek, A.M. Michałowska-Kaczmarczyk, A.G. Asuero, New trends in studies on electrolytic redox systems, Electrochimica Acta 109 (2013) 519-531.
[47] S. Chio, J.S. Hyde, R.C. Sealy, Paramagnetism in Melanins: pH Dependence, Archives of Biochemistry and Biophysics 215 (1982) 100-106.
[48] S. Steenken, P. Neta, Electron Transfer Rates and Equilibria between Substituted Phenoxide Ions and Phenoxyl Radicals, Journal of Physical Chemistry 83 (1979) 1134-1137.
[49] Y.A. Ilan, G. Czapski, D. Meisel, The one electron transfer redox potentials of free radicals, Biochemica Biophysica Acta 430 (1976) 209-224.
[50] Y. Han, C. Jin, Computational screening of electroactive indolequinone derivatives as high performance active materials for aqueous redox flow batteries, Current Applied Physics 18 (2018) 1507-1512.
[51] C.L. Serpentini, C. Gauchet, D. de Montauzon, M. Comtat, J. Ginestar, N. Paillous, First electrochemical investigation of the redox properties of DOPA–melanins by means of a carbon paste electrode, Electrochimica Acta 45 (2000) 1663–1668.
[52] V. Horak, J.R. Gillette, A Study of the Oxidation-Reduction State of Synthetic 3,4-Dihydroxy-DL-phenylalanine Melanin, Molecular Pharmacology 7 (1971) 429-433.
[53] L. Chauffe, J.J. Windle, M. Friedman, Electron Spin Resonance Study of Melanin Treated with Reducing Agents, Biophysical Journal 15 (1975) 565-572.
[54] T.G. Costa, R. Younger, C. Poe, P.J. Farmer, B. Szpoganicz, Studies on Synthetic and Natural Melanin and Its Affinity for Fe(III) Ion, Bioinorganic Chemistry and Applications 2012 (2012) 712840.
[55] L.K. Charkoudian, J.F. Katherine, Fe(III)-Coordination Properties of Neuromelanin Components: 5,6-Dihydroxyindole and 5,6-Dihydroxyindole-2-carboxylic Acid, Inorganic Chemistry 45 (2006) 3657-3664.
[56] A.T. AI-Kazwini, P. O'Neill, G.E. Adams, R.B. Cundall, B. Jacquet, G. Lang, A. Junino, One-Electron Oxidation of Methoxylated and Hydroxylated Indoles by N3'. 1. Characterization of the Primary Indolic Radicals, Journal of Physical Chemistry 94 (1990) 6666-6670.
[57] A.J. Swallow, Physical Chemistry of Semiquinones, in: B.L. Trumpower (Ed.), Function of Quinones in Energy Conserving Systems, Academic Press1982, pp. 608.
[58] T.E. Young, J.R. Griswold, M.H. Hulbert, Melanin. I. Kinetics of the Oxidative Cyclization of Dopa to Dopachrome, Journal of Organic Chemistry 39 (1974) 1980-1982.
[59] M. Liu, S. Han, X. Zheng, L. Han, T. Liu, Z. Yu, Experimental and Theoretical Prediction of The Redox Potential of Dopamine and Its Supramolecular Complex With Glycine, International Journal of Electrochemical Science 10 (2015) 235-247.
[60] T. Liu, L. Han, C. Du, Z. Yu, Redox Potentials of Dopamine and Its Supramolecular Complex with Aspartic Acid, Russian Journal of Physical Chemistry A 88 (2014) 1085-1090.
[61] S. Chen, K.T. Peng, The electrochemical properties of dopamine, epinephrine, norepinephrine, and their electrocatalytic reactions on cobalt(II) hexacyanoferrate films, Journal of Electroanalytical Chemistry 547 (2003) 179-189.
[62] M. Uchimiya, A.T. Stone, Redox reactions between iron and quinones: Thermodynamic constraints, Geochimica et Cosmochimica Acta 70 (2006) 388–1401.
[63] T. Michałowski, Application of GATES and MATLAB for Resolution of Equilibrium, Metastable and Non-Equilibrium Electrolytic Systems, in: T. Michałowski (Ed.), Applications of MATLAB in Science and Engineering, InTech2011, pp. 510.
[64] V. Horak, G. Weeks, Poly(5,6-dihydroxyindole) Melanin Film Electrode, Bioorganic Chemistry 21 (1993) 24-33.
[65] Z. Tehrani, S.P. Whelan, B. Mostert, J.V. Paulin, M.M. Ali, E.D. Ahmadi, C.F.O. Graeff, O.J. Guy, D.T. Gethin, Printable and Flexible Graphene pH sensors utilising Thin Film Melanin for Physiological Applications, 2D Materials 7 (2020) 024008.
[66] T.G. Costa, B. Szpoganicz, G.F. Caramori, V.R. de Almeida, A.S. Mangrich, A.P. Mangoni, Spectroscopy and theoretical studies of natural melanin (eumelanin) and its complexation by iron(III), Journal of Coordination Chemistry 67 (2014) 986-1001.
[67] S. Chio, J.S. Hyde, R.C. Sealy, Temperature-Dependent Paramagnetism in Melanin Polymers, Archives of Biochemistry and Biophysics 199 (1980) 133-139.

[68] F.W. Cope, R.J. Sever, B.D. Polis, Reversible Free Radical Generation in the Melanin Granules of the Eye by Visible Light, Archives of Biochemistry and Biophysics 100 (1963) 171-177.
[69] F.J. Grady, D.C. Borg, Electron Paramagnetic Resonance Studies on Melanins 1. The Effect of pH on Spectra at Q-band, Journal of the American Chemical Society 90 (1968) 2949-2952.
[70] M. Pasenkiewicz-Gierula, R.C. Sealy, Analysis of the ESR Spectrum of Synthetic DOPA Melanin., Biochimica et Biophysica Acta 884 (1986) 510-516.
[71] B.L.L. Seagle, K.A. Rezai, E.M. Gasyna, Y. Kobori, K.A. Rezaei, J.R. Norris Jr., Time-Resolved Detection of Melanin Free Radicals Quenching Reactive Oxygen Species, Journal of the American Chemical Society 127 (2005) 11220-11221.
[72] T. Sarna, H.A. Swartz, The Physical Properties of Melanin, in: J.J. Nordlund, R.E. E. Boissy, V.J. Hearing, R.A. King, W.S. Oetting, J. Ortonne (Eds.), The Pigmentary System: Physiology and Pathophysiology, Blackwell Publishing2006.
[73] M. Uchimiya, A.T. Stone, Reversible redox chemistry of quinones: Impact on biogeochemical cycles, Chemosphere 77 (2009) 451–458.
[74] L. Panzella, G. Gentile, G. D'Errico, N.F. Della Vecchia, M.E. Errico, A. Napolitano, C. Carfagna, M. d'Ischia, Atypical Structural and π-Electron Features of a Melanin Polymer That Lead to Superior Free-Radical-Scavenging Properties, Angewandte Chemie International Edition 52 (2013) 12684-12687.